

RESEARCH

Open Access



Bacterial sepsis causes more dramatic pathogenetic changes in the Th1 pathway than does viral (COVID-19) sepsis: a prospective observational study of whole blood transcriptomes

Arisa Muratsu^{1†}, Sayaka Oda^{2,3†}, Shinya Onishi^{1†}, Jumpei Yoshimura^{1†}, Hisatake Matsumoto^{1*}, Yuki Togami¹, Yumi Mitsuyama¹, Hiroshi Ito¹, Daisuke Okuzaki³, Hiroshi Ogura¹ and Jun Oda¹

Abstract

Objectives This study aimed to comprehensively compare host responses of patients with bacterial sepsis and those with viral (COVID-19) sepsis by analyzing messenger RNA (mRNA) and microRNA (miRNA) profiles to shed light on their distinct pathophysiological mechanisms.

Design Prospective observational study.

Setting Whole blood RNA sequencing was used to analyze mRNA and miRNA profiles of patients diagnosed as having bacterial sepsis or viral (COVID-19) sepsis at the Department of Trauma and Emergency Medicine, Osaka University Graduate School of Medicine.

Patients Twenty-two bacterial sepsis patients, 35 viral (COVID-19) sepsis patients, and 15 healthy subjects admitted to the department were included. We diagnosed bacterial sepsis patients according to the sepsis-3 criterion that the Sequential Organ Failure Assessment score must increase to 2 points or more among patients with suspected infections. Viral (COVID-19) sepsis patients were diagnosed using SARS-CoV-2 RT-PCR testing, and presence of pneumonia was assessed through chest computed tomography scans.

Interventions None.

Measurements and main results For RNA sequencing, 14,500 mRNAs, 1121 miRNAs, and 2556 miRNA-targeted mRNAs were available for analysis in the bacterial sepsis patients. Numbers of genes showing upregulated: downregulated gene expression (false discovery rate < 0.05, |log₂ fold change| > 1.5) were 256:2887 for mRNA,

[†]Arisa Muratsu, Sayaka Oda, Shinya Onishi and Jumpei Yoshimura contributed equally to this work.

*Correspondence:
Hisatake Matsumoto
h-matsumoto@hp-emerg.med.osaka-u.ac.jp

Full list of author information is available at the end of the article



© The Author(s) 2024. **Open Access** This article is licensed under a Creative Commons Attribution-NonCommercial-NoDerivatives 4.0 International License, which permits any non-commercial use, sharing, distribution and reproduction in any medium or format, as long as you give appropriate credit to the original author(s) and the source, provide a link to the Creative Commons licence, and indicate if you modified the licensed material. You do not have permission under this licence to share adapted material derived from this article or parts of it. The images or other third party material in this article are included in the article's Creative Commons licence, unless indicated otherwise in a credit line to the material. If material is not included in the article's Creative Commons licence and your intended use is not permitted by statutory regulation or exceeds the permitted use, you will need to obtain permission directly from the copyright holder. To view a copy of this licence, visit <http://creativecommons.org/licenses/by-nc-nd/4.0/>.

53:5 for miRNA, and 49:2507 for miRNA-targeted mRNA. Similarly, in viral (COVID-19) sepsis patients, 14,500 mRNAs, 1121 miRNAs, and 327 miRNA-targeted mRNAs were analyzed, with numbers of genes exhibiting upregulated: downregulated gene expression of 672:1147 for mRNA, 3:4 for miRNA, and 165:162 for miRNA-targeted mRNA. This analysis revealed significant differences in the numbers of upregulated and downregulated genes expressed and pathways between the bacterial sepsis and viral (COVID-19) sepsis patients. Bacterial sepsis patients showed activation of the PD-1 and PD-L1 cancer immunotherapy signaling pathway and concurrent suppression of Th1 signaling.

Conclusion Our study illuminated distinct molecular variances between bacterial sepsis and viral (COVID-19) sepsis. Bacterial sepsis patients had a greater number of upregulated and downregulated genes and pathways compared to viral (COVID-19) sepsis patients. Especially, bacterial sepsis caused more dramatic pathogenetic changes in the Th1 pathway than did viral (COVID-19) sepsis.

Keywords COVID-19, PD-1 and PD-L1 cancer immunotherapy signaling pathways, Bacterial sepsis, Th1 signaling, Whole blood transcriptome

Introduction

Bacterial sepsis and viral (COVID-19) sepsis are severe and life-threatening infectious diseases that necessitate intensive care [1–3]. Despite their clinical significance, the underlying pathophysiological mechanisms in these conditions remain inadequately understood, and a comprehensive comparison of their host responses is lacking. Understanding the molecular alterations and immune responses occurring in the body is crucial for improving diagnostic and therapeutic approaches.

Noncoding RNA (ncRNA), which is not translated into protein, accounts for about 98% of all RNA. Among ncRNAs, microRNAs (miRNAs) regulate translational repression and messenger RNA (mRNA) degradation by binding to the 3' untranslated region of target mRNAs. Through these mechanisms, miRNAs contribute to the fine-tuning of gene expression networks that underlie diverse biological functions [4, 5].

Therefore, the purpose of this study was to integrate mRNA and miRNA data in whole blood of patients with acute bacterial sepsis and patients with viral (COVID-19) sepsis to compare the differences in host responses between bacterial sepsis and viral (COVID-19) sepsis and to better understand the pathophysiology of each.

Materials and methods

Study design and setting

This was a single-center, prospective, observational study. This study was performed at the Department of Traumatology and Acute Critical Medicine, Graduate School of Medicine, Osaka University. The study period was the 8 months from July 1, 2020, to February 28, 2021.

Participants

We included the bacterial sepsis patients and viral (COVID-19) sepsis patients who were admitted to the department during the study period. We diagnosed them

as having bacterial sepsis or viral (COVID-19) sepsis according to the sepsis-3 criterion that the Sequential Organ Failure Assessment (SOFA) score be increased to 2 points or more among patients with suspected infections [6]. Viral (COVID-19) sepsis patients were also diagnosed using SARS-CoV-2 RT-PCR testing, and the presence of pneumonia was assessed through chest computed tomography scans. Blood samples were obtained from the patients on hospital admission and once from healthy volunteers who were enrolled via public poster advertisements.

Clinical data

Clinical data collected from the patients' electronic medical records by the investigators included age, sex, body mass index, comorbidities, mechanical ventilation, length of hospital stay, mortality, and severity. We evaluated the severity of bacterial sepsis and viral (COVID-19) sepsis in the patients with the Acute Physiology and Chronic Health Evaluation II (APACHE II) and SOFA scores. We collected information regarding the underlying infection causing bacterial sepsis and the presence of hypotension from the bacterial and viral (COVID-19) sepsis patients. We also used the Acuity Score to define the severity of COVID-19 [7]. We defined the patients whose systolic blood pressure was less than 90 mmHg on hospital admission as having hypotension. The oxygenation index was calculated as the P/F ($\text{PaO}_2/\text{FiO}_2$ [fraction of inspired oxygen]) ratio. Liver and kidney organ indices were collected from APACHE II and SOFA score items, and bilirubin for liver function and creatinine for renal function were selected. The following five items were selected for supportive care: ventilator (with or without intubation), CRRT (continuous renal replacement therapy), steroids (hydrocortisone sodium succinate for septic shock), ECMO (extracorporeal membrane oxygenation), and catecholamine.

Identification of mRNA and miRNA expressions

Total RNA isolation of leukocytes was performed using blood obtained from the bacterial sepsis patients and viral (COVID-19) sepsis patients on hospital admission and from the healthy controls using the PAXgene™ Blood RNA System (BD Bioscience, San Jose, CA). Blood samples for the analyses were obtained using collection tubes and preserved at -30 °C until subsequent analysis. To prepare the libraries, the TruSeq Stranded mRNA Sample Prep Kit (Illumina, San Diego, CA) was used by following the manufacturer's instructions.

Library preparation and RNA sequencings

Full-length cDNA was prepared using a SMART-Seq HT Kit (Takara Bio, Mountain View, CA) according to the manufacturer's instructions. An Illumina library was prepared using a Nextera DNA Library Preparation Kit (Illumina) according to the SMARTer kit instructions. DNA libraries were converted to libraries for DNBSEQ using an MGIEasy Universal Library Conversion Kit (App-A). Sequencing was performed on a DNBSEQ-G400RS platform in 2×100 bp paired-end mode.

RNA-seq analysis

The analysis was performed with some modifications as shown in a previous article [7]. The sequenced reads were aligned to the human reference genome sequences (hg19) using TopHat (version 2.1.1) in conjunction with Bowtie2 (version 2.2.8) and SAMtools (version 0.1.18). Raw read counts of gene-level expression were determined with featureCounts using the subread-2.0.0 package.

miRNA sequencing and miRNA-seq analysis

This analysis was performed with some modifications as shown in a previous article [7]. Small RNA libraries were prepared using the NEBNext Small RNA Library Prep Set for Illumina (New England Biolabs, Ipswich, MA) according to the manufacturer's instructions. miRNAs were sequenced on a NovaSeq 6000 platform (Illumina) in 101-bp single-end reads. Prior to conducting analysis on the small RNA-Seq data, a preprocessing step was carried out involving the removal of the 3' adapter sequence (AGATCGGAAGAGCACACGTCT) from the reads. Subsequently, the processed reads were aligned against both the miRBase human miRNA dataset and the FANTOM5 dataset utilizing miRDeep2 software. Quantification of expression was also executed using the miRDeep2 software package.

Statistical analysis of mRNA and miRNA

Gene activity signatures provide the optimal bar code to characterize the kind and status of a living system (cell, tissue, organ, or organism). These signatures can be used as they are, just as a marker for a certain phenomenon of

interest, e.g., as a biomarker of a specific disease [8]. For a more refined inspection of the biological semantics of the observed expression pattern, differentially expressed genes (DEGs) are identified by comparing gene activity spectra of the cellular system of interest and a control cell [8]. Because the regulation of gene expression, mainly at the transcriptional but also at post-transcriptional level, is involved in nearly any biological process, most standard analyses of transcriptome data usually comprise mapping of DEG sets to Gene Ontology (GO) categories, for instance by GSEA (gene set enrichment analysis) [8]. Regulatory or metabolic pathways that are enhanced by the DEGs can be identified by mapping them onto the pathway databases. The pathway analysis used in this study is categorized as a conventional approach called "downstream analysis" and provides relevant insights into the effects of the induced genes [8]. However, it provides only very limited clues as to the cause of the observed effects. Therefore we added an "upstream analysis" that allows causal interpretation of observed expression changes. This comprises a state-of-the-art analysis of the promoter structures of the identified DEGs, infers the involved transcription factors, and identifies the signaling pathways that activate these transcription factors. In a final step, convergence points of these pathways are identified as potential master regulators or key nodes [8].

Extraction of mRNA and miRNAs with significant gene expression changes

The analysis was performed with some modifications as shown in a previous article [7]. We normalized mRNA raw count data using integrated Differential Expression and Pathway analysis ver. 0.96. Normalization settings were min.CPM=0.5, n libraries=5. It has been reported that variation in sequencing depth between libraries had a noticeable impact on some RNA-Seq analysis methods. Therefore, we chose limma-voom analysis [9] to search for differentially expressed genes of bacterial sepsis and viral (COVID-19) sepsis patients based on the healthy controls. Principal component analysis (PCA) in R was performed to compare gene expression among patients with bacterial sepsis and those with viral (COVID-19) sepsis and in the healthy controls. Then, volcano plot analysis was performed to visualize and identify significant changes in the gene expression list. In this study, cut-off values were set at a false discovery rate (FDR) < 0.05 and $|\log_2 \text{fold change}| > 1.5$. The raw count data for miRNAs were processed in the same manner.

Canonical pathway analysis and upstream regulator analysis

The analysis was performed with some modifications as shown in a previous article [7]. DEGs were identified in the bacterial sepsis patients vs. healthy controls and in the viral (COVID-19) sepsis patients vs. healthy controls,

and canonical pathway analysis and upstream regulator analysis were performed. The goal of canonical pathway analysis is to identify biological functions (pathways) that are expected to increase or decrease based on the changes in gene expression observed in our data set. The goal of the upstream regulator analysis is to identify a cascade of upstream transcriptional regulators that can explain the gene expression changes observed in our data set. The analysis was performed using Ingenuity Pathway Analysis (IPA) software (QIAGEN Inc., <https://digitalinsights.qiagen.com/products-overview/discovery-insights-portfolio/analysis-and-visualization/qiagen-ipa/>) with the Ingenuity Knowledge Base, which is based on a large number of previous reports. The Benjamini-Hochberg method was used to correct for significance level.

In the case of canonical pathways, the z -score is interpreted by calculating the predicted value of whether the pathway is active or not based on the expression levels of each RNA involved in a specific biological function (pathway). If the pathway is predicted to be active, $z > 0$, and if it is predicted to be repressed, $z < 0$. The concept is similar for z -score in the case of upstream regulator analysis. The expression levels of some genes are controlled by transcriptional regulators. The upstream RNAs controlling the identified DEGs are identified, and $z > 0$ if there are more predictions that the regulating RNAs are active based on the gene expression levels of the DEGs. If the absolute value of the z -score is greater than 2, it is considered significant. The adjusted p value in canonical pathway analysis indicates how much the DEGs are included in the components of a particular pathway, and the more highly related that pathway is, the lower the value. Significance is indicated by an adjusted p value < 0.05 . The overlap of p values in upstream regulator analysis indicates whether there is a statistically significant overlap between the DEGs identified in this study and the genes regulated by the transcriptional regulators. This is calculated using Fisher's exact test, and significance is indicated by a p value < 0.01 . Predicted miRNA-targeted mRNA expression was obtained from IPA using miRecords, TarBase, and TargetScan as miRNA-targeted mRNA expression databases.

Continuous values are shown as median and interquartile range (IQR), and categorical variables are shown using frequencies and proportions. Comparisons were performed using the nonparametric Mann-Whitney test as appropriate. No imputation was made for missing data. A value of $p < 0.05$ was considered to indicate statistical significance. The data were analyzed using JMP Pro version 16.0.0 (SAS Institute, Cary, NC). The workflow of this research is shown in Fig. 1.

Results

Patient characteristics

We included 22 bacterial sepsis patients, 35 viral (COVID-19) sepsis patients, and 15 healthy controls. Table 1 shows the baseline patient characteristics of this study. The median ages of the bacterial sepsis patients, viral (COVID-19) sepsis patients, and healthy controls were 77.5 (IQR 65.3–82.0), 72.0 (IQR 59.0–76.0), and 55 (IQR 40.5–59.0) years, and 72.7%, 70.6%, and 68.6% were male, respectively. There was a statistically significant difference in age between the three groups but no statistically significant differences in gender and body mass index. All bacterial sepsis patients had bacterial infection, were negative for COVID-19 on admission, and had no prior infection. We diagnosed COVID-19 patients with the acuity score [7]: 1=death: 4 (11.4%) patients, 2=intubated/ventilated, survived: 26 (74.3%) patients, 3=hospitalized, O₂ required, survived: 3 (14.3%) patients, 4=hospitalized, no O₂ required, survived: 0 (0%) patients, and 5=discharged/not hospitalized, survived: 0 (0%) patients.

The median lengths of hospital stay for the bacterial sepsis patients and viral (COVID-19) sepsis patients were 16.5 (IQR 4.8–35.8) and 12.0 (IQR 6.5–25.5) days, and the mortality rates during hospitalization for the bacterial sepsis and viral (COVID-19) sepsis patients were 13.6% and 11.4%, respectively.

The median SOFA scores on admission for the bacterial sepsis and viral (COVID-19) sepsis patients were 7 (IQR 4.0–11.3) and 5 (IQR 3–7), and median APACHE II scores were 16.5 (IQR 14.0–23.8) and 14.0 (IQR 10.0–19.0), respectively.

The most common source of bacterial sepsis was the respiratory system (68.2%), followed by abdomen (4.5%), urinary tract (9.1%), soft tissue (9.1%), and others (9.1%). Seven bacterial sepsis patients (7.0%) and 2 viral (COVID-19) sepsis patients (5.7%) had hypotension. Patient characteristics are shown in Table 1.

Whole blood RNA sequence

For RNA sequencing, 4500 mRNAs, 1121 miRNAs, and 2556 miRNA-targeted mRNAs were available for analysis in the patients diagnosed as having bacterial sepsis. Within this dataset, the numbers of genes with varying levels of upregulated: downregulated gene expression (FDR < 0.05 , $|\log_2$ fold change| > 1.5) were 256:2887 for mRNA, 53:5 for microRNA, and 49:2507 for miRNA-targeted mRNA (Fig. 2A, B). Similarly, in the context of viral (COVID-19) sepsis patients, 14,500 mRNAs, 1121 miRNAs, and 327 miRNA-targeted mRNAs were subjected to analysis, with the numbers of genes exhibiting variation in upregulated: downregulated gene expression being 672:1147 for mRNA, 3:4 for microRNA, and 165:162 for miRNA-targeted mRNA (Fig. 2C, D). PCA

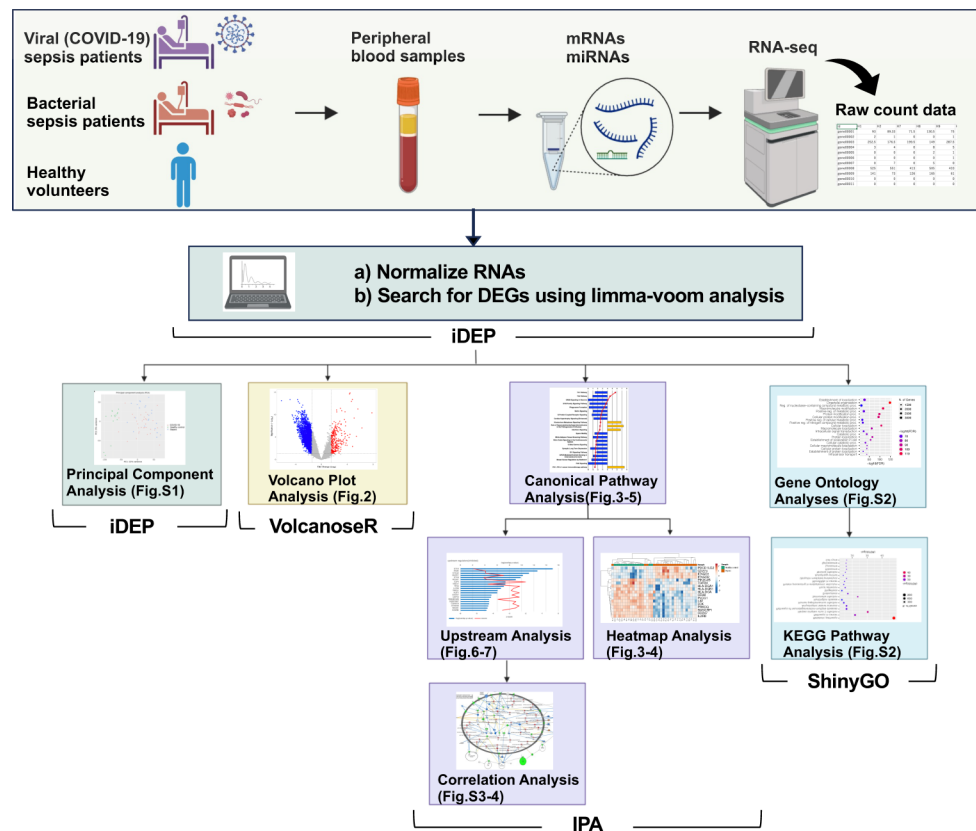


Fig. 1 Workflow of our research. DEGs, differentially expressed genes; iDEP, integrated Differential Expression and Pathway analysis; IPA, Ingenuity Pathway Analysis

indicated that mRNA and miRNA profiles could be used to differentiate individuals with bacterial sepsis from those with viral (COVID-19) sepsis and healthy controls to a certain degree (Fig. S1A, B).

Canonical pathway analysis of patients with bacterial sepsis and healthy controls

The mRNA-based analysis revealed 11 pathways that were dynamically differentiated in bacterial sepsis patients compared to healthy controls, with both the adjusted p value and z-score significant (Fig. 3A). The adjusted p value for the PD-1 and PD-L1 cancer immunotherapy pathway was $4.4E-06$ and z-score=2.89. In the downregulated pathways, the adjusted p value for the Th1 pathway was the lowest (adjusted p value= $4.0E-14$, z-score = -5.69). Figure 3B shows the percentage of genes up- and down-regulated in the 11 pathways shown in Fig. 3A. These charts display the number of molecules in our dataset that belong to a significant pathway and show the proportions of up-regulated (orange), and down-regulated (green) molecules. Figure 3C shows a heatmap of genes in the PD-1 and PD-L1 cancer immunotherapy pathways as representatives of the upregulated pathways and how each gene is upregulated and downregulated. Thirty-three mRNAs were involved in the PD-1 and

PD-L1 cancer immunotherapy pathway. Figure 3D shows a heatmap of genes in the Th1 pathway as a representative of down-regulated pathways and how each gene is up- and down-regulated. Forty-nine mRNAs were involved in the Th1 pathway. In addition, two types of GSEA, GO analysis and Kyoto Encyclopedia of Genes and Genomes (KEGG) pathway analysis, were used to prove these IPA analyses. Figure S2A-D shows that similar results are confirmed for pathway analysis results other than by IPA.

Canonical pathway analysis of viral (COVID-19) sepsis patients and healthy controls

Based on mRNA, 21 pathways were differentiated in viral (COVID-19) sepsis patients compared to the healthy controls (Fig. 4A). The adjusted p value for the PD-1 and PD-L1 cancer immunotherapy pathway was $3.69E-02$ and z-score=3.5. In the downregulated pathways, the adjusted p value for the Th1 pathway was the lowest (adjusted p value= $2.33 E-06$, z-score = -2.57).

As with bacterial sepsis, Fig. 4B shows the percentage of genes up- and down-regulated in the 21 pathways shown in Fig. 4A. Figure 4C shows a heatmap of genes in the PD-1 and PD-L1 cancer immunotherapy pathways as representatives of the upregulated pathways, and how each gene is upregulated and downregulated. Eighteen

Table 1 Baseline characteristics of bacterial sepsis patients, viral (COVID-19) sepsis patients, and healthy controls

| Baseline characteristics | Bacterial sepsis patients (N=22) | Viral (COVID-19) sepsis Patients (N=35) | Healthy controls (N=15) | p-Value |
|--|---|--|------------------------------------|----------------|
| Age, years, median (IQR) | 77.5(65.3-82.0) | 72(59.0-76.0) | 55(40.5-59.0) | < .001 |
| Male, n (%) | 16(72.7) | 24(68.6) | 8(50.0) | 0.46 |
| BMI, median (IQR) | 22.1(20.2-26.2) | 23.2(22.6-25.4) | 22(20.5-24.2) | 0.67 |
| Comorbidities, n (%) | | | | |
| Diabetes | 2(9.0) | 11 (31.4) | 1 (6.3) | |
| Hypertension | 8 (36.4) | 16(45.7) | 2 (12.5) | |
| Hyperlipidemia | 3(13.6) | 5(14.3) | 6 (37.5) | |
| Chronic lung disease | 0(0) | 6 (17.1) | 0 (0) | |
| Chronic kidney disease | 1(4.5) | 9 (25.7) | 0 (0) | |
| Immunocompromised condition | 4(18.2) | 4 (11.4) | 0 (0) | |
| Focus of sepsis, n (%) | | | | |
| Respiratory system | 15(68.2) | 35(100) | | |
| Abdomen | 1(4.5) | 0(0) | | |
| Urinary tract | 2(9.1) | 0(0) | | |
| Soft tissue | 2(9.1) | 0(0) | | |
| Others | 2(9.1) | 0(0) | | |
| Mechanical ventilation, n (%) | 17 (77.2) | 30 (85.7) | | |
| Liver and renal function evaluation | | | | |
| P/F ratio | 166 | 181 | | |
| Bilirubin | 1 | 1 | | |
| Creatinine | 1 | 1 | | |
| Severity of disease on admission | | | | |
| SOFA score, median (IQR) | 7(4.0-11.3) | 5(3-7) | | |
| APACHE II score, median (IQR) | 16.5(14.0-23.8) | 14.0(10.0-19.0) | | |
| Acuity Score (for COVID-19 patients), n (%) | | | | |
| 1 = Death | | 4(11.4) | | |
| 2 = Intubated/ventilated, survived | | 26(74.3) | | |
| 3 = Hospitalized, O ₂ required, survived | | 3(14.3) | | |
| 4 = Hospitalized, no O ₂ required, survived | | 0(0) | | |
| 5 = Discharged/not hospitalized, survived | | 0(0) | | |
| Treatment* | | | | |
| Catecholamine | 12 | 22 | | |
| CRRT | 6 | 3 | | |
| Steroid (for shock) | 8(36.4) | 0(0) | | |
| ECMO | 0 | 1 | | |
| Disease course | | | | |
| Hypotension, n (%) | 7 | 2(5.7) | | |
| Length of hospital stay, days, median (IQR) | 16.5 (4.8-35.8) | 12.0(6.5-25.5) | | |
| Hospital mortality, n (%) | 3 (13.6) | 4(11.4) | | |

IQR, interquartile range; BMI, body mass index; SOFA, Sequential Organ Failure Assessment; APACHE, Acute Physiology and Chronic Health Evaluation; P/F ratio, PaO₂/fraction of inspired oxygen (FiO₂) ratio; CRRT, continuous renal replacement therapy; ECMO, extracorporeal membrane oxygenation. There are missing data in patients with bacterial sepsis (BMI, bilirubin) and patients with viral sepsis (BMI, P/F ratio). We used the median imputation method, imputation of missing values using the population median for continuous predictors, or the population mean proportion for categorical predictors derived from the data in which the risk score was originally developed. The *p* values for age, gender, and BMI were each calculated from a one-way analysis of variance. The Acuity Score was used to assess severity in patients with viral (COVID-19) sepsis.

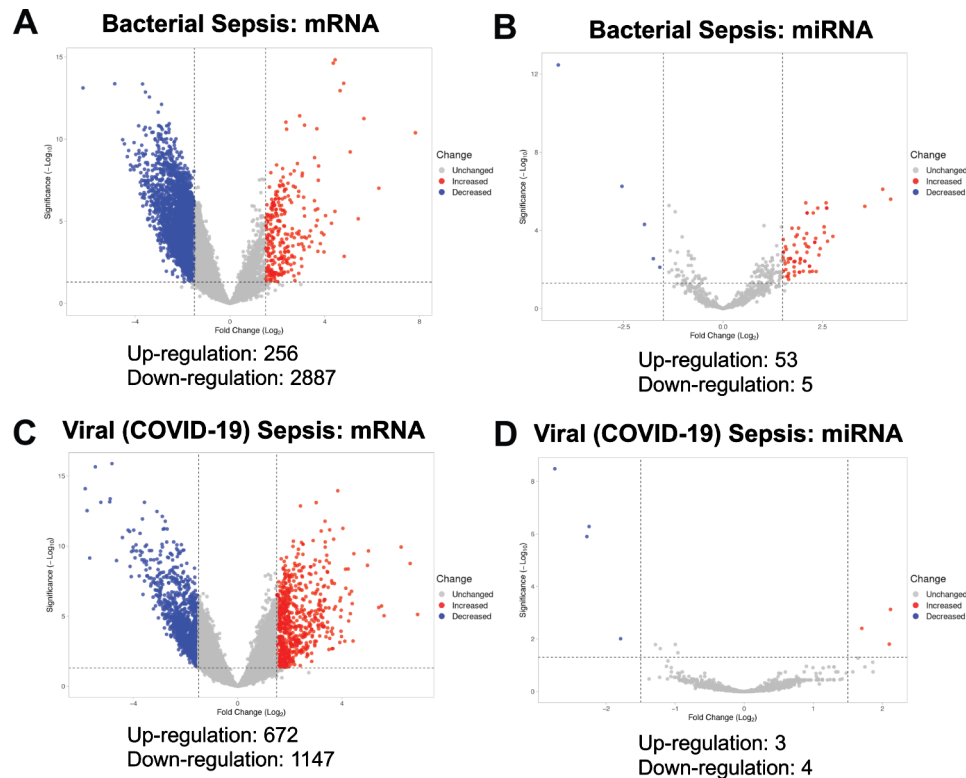


Fig. 2 Gene expression variation analysis of total mRNA and miRNA. Gene expression variation analysis representing mRNA expression (**A**) and miRNA expression (**B**) specifically expressed in bacterial sepsis patients compared to healthy controls. (**C**) Gene expression variation analysis representing mRNA expression (**C**) and miRNA expression (**D**) specifically expressed in viral (COVID-19) sepsis patients compared to healthy controls. The vertical dotted lines represent $|\log_2 \text{fold change}| > 1.5$, and the horizontal dotted line represents the threshold for $FDR < 0.05$. Red dots indicate RNAs with increased expression and blue dots indicate RNAs with decreased expression

mRNAs were involved in the PD-1 and PD-L1 cancer immunotherapy pathway. Figure 4D shows a heatmap of genes in the Th1 pathway as a representative of down-regulated pathways and how each gene is up- and down-regulated. Thirty-one mRNAs were involved in the Th1 pathway.

Analysis based on miRNA-targeted mRNAs in bacterial sepsis patients showed 11 pathways that were differentiated (Fig. 5A). The adjusted p value for the PD-1 and PD-L1 cancer immunotherapy pathway was $4.41E-06$ and $z\text{-score}=2.89$. In the downregulated pathways, the adjusted p value for the Th1 pathway was the lowest (adjusted p value= $4.33 E-14$, $z\text{-score} = -5.69$). As with bacterial sepsis, Fig. 5B shows the percentage of genes up- and down-regulated in the 11 pathways shown in Fig. 5A.

Analysis based on miRNA-targeted mRNAs in viral (COVID-19) sepsis patients showed only one active pathway, p38 MAPK Signaling (adjusted p value= $1.1E-02$, $z\text{-score}=2.33$) (Fig. 5C). There were no significant pathways that were suppressed. As with bacterial sepsis, Fig. 5D shows the percentage of genes up- and down-regulated in the 11 pathways shown in Fig. 5C. Here also, GO analysis and KEGG pathway analysis were used to

prove these IPA analyses. Figure S2E-H shows that similar results are confirmed for pathway analysis results other than by IPA.

Upstream regulator analysis of patients with bacterial sepsis and healthy controls

Based on the mRNAs that were significantly differentially expressed in the septic patients compared to healthy controls, there were 1559 active factors regulating transcription of these mRNAs (top 20 regulators are shown in Fig. 6A). The number of inhibited transcriptional regulators was 125 (top 20 regulators are shown in Fig. 6B). Based on miRNA-targeted mRNAs, 1844 transcriptional regulators were significantly activated (top 20 regulators are shown in Fig. 6C), and 149 regulators were suppressed (top 20 regulators are shown in Fig. 6D).

Upstream regulator analysis of viral (COVID-19) sepsis patients and healthy controls

Based on the mRNAs that were significantly differentially expressed in the viral (COVID-19) sepsis patients compared to the healthy controls, there were 65 factors regulating transcription of those mRNAs that were active (top 20 regulators are shown in Fig. 7A). There were 32

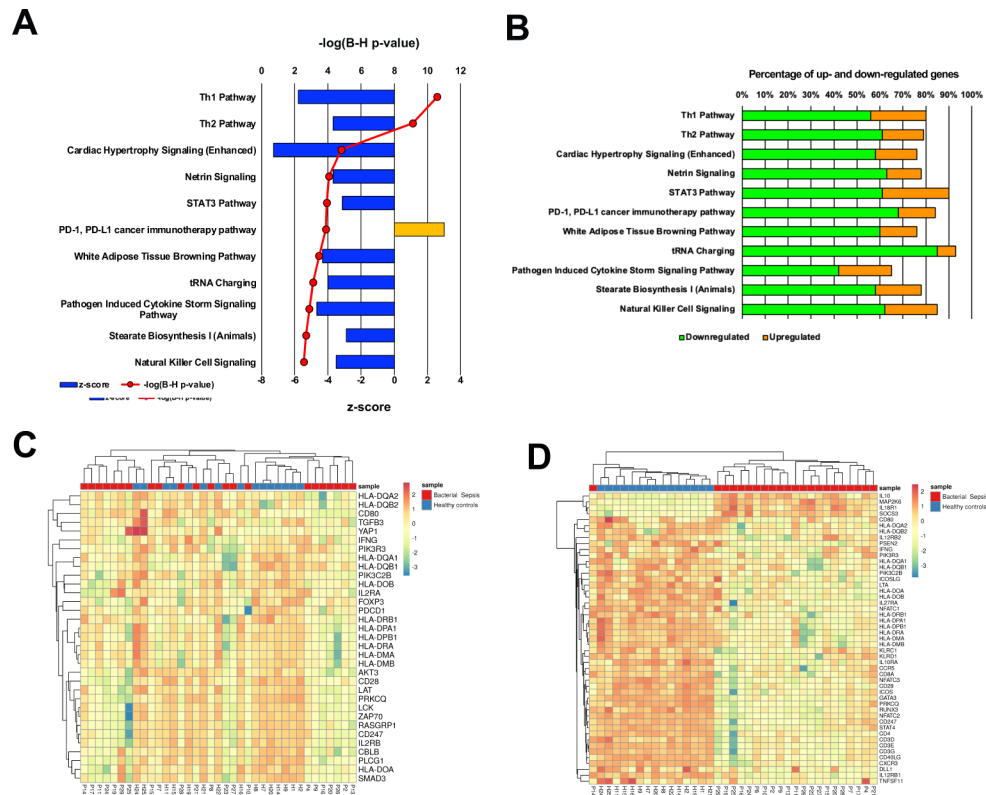


Fig. 3 Canonical pathway and heatmaps of mRNA in patients with bacterial sepsis. **(A)** Canonical pathway analysis of patients with bacterial sepsis and healthy volunteers. The bars represent z-scores, and the line graphs represent the adjusted p values associated with each pathway in the logarithm. **(B)** The percentage of genes up- and down-regulated in the pathways shown in panel A. These charts display the number of molecules in our dataset that belong to a significant pathway and show the proportions of upregulated (orange) and downregulated (green) molecules. **(C)** A heatmap of genes in the PD-1 and PD-L1 cancer immunotherapy pathways as representatives of the upregulated pathways, and how each gene is upregulated and down-regulated. **(D)** A heatmap of genes in the Th1 pathway as a representative of downregulated pathways, and how each gene is up- and down-regulated

inhibited transcriptional regulators (top 20 regulators are shown in Fig. 7B). Analysis using miRNA-targeted mRNAs revealed 18 active transcriptional regulators (Fig. 7C) and seven significantly inhibited transcriptional regulators (Fig. 7D).

Canonical signaling pathway analysis of patients with bacterial sepsis and healthy controls

The mRNA-miRNA integration analyses by IPA are shown in Figs. S3 and S4. Fig. S3 shows the predicted relationship between RNAs in the activated PD-1 and PD-L1 cancer immunotherapy signaling pathway. PD-1, PD-L1 cancer immunotherapy signaling involved 46 miRNAs. Fig. S4 shows the predicted relationship between RNAs in the inhibited Th1 pathway. Th1 signaling was predicted to involve 50 miRNAs.

Discussion

A previous study examining bacterial sepsis and viral (COVID-19) sepsis [10] included 64 patients with bacterial sepsis and 43 with severe acute respiratory syndrome coronavirus 2 (SARS-CoV-2) sepsis. The results of routine blood tests (neutrophil, lymphocyte, and monocyte

counts), infection biomarkers (C-reactive protein, ferritin, and procalcitonin levels), lymphocyte subset counts (total T lymphocyte, CD4+ and CD8+ T-cell, B-cell, and NK-cell counts), and lymphocyte subset functions (proportions of PMA/ionomycin-stimulated IFN- γ -positive cells in CD4+ and CD8+ T cells and NK cells) were similar in both patient groups. Cytokine storm was milder and immunoglobulin and complement protein levels were higher in the SARS-CoV-2 sepsis patients.

We focused on this comparison and compared the results of transcriptome analysis to elucidate the differences between bacterial and viral sepsis. The number of genes with variable expression is shown in Fig. 2A-D. mRNAs showed 3143 DEGs in bacterial sepsis and 1819 DEGs in viral (COVID-19) sepsis patients. miRNAs showed 58 DEGs in bacterial sepsis and only 7 in viral sepsis. These results indicate that gene expression is much higher in bacterial sepsis.

PCA allowed us to distinguish septic patients from viral (COVID-19) sepsis patients and healthy controls to some extent. Bacterial sepsis patients had a greater number of upregulated and downregulated genes and pathways compared to the viral (COVID-19) sepsis patients,

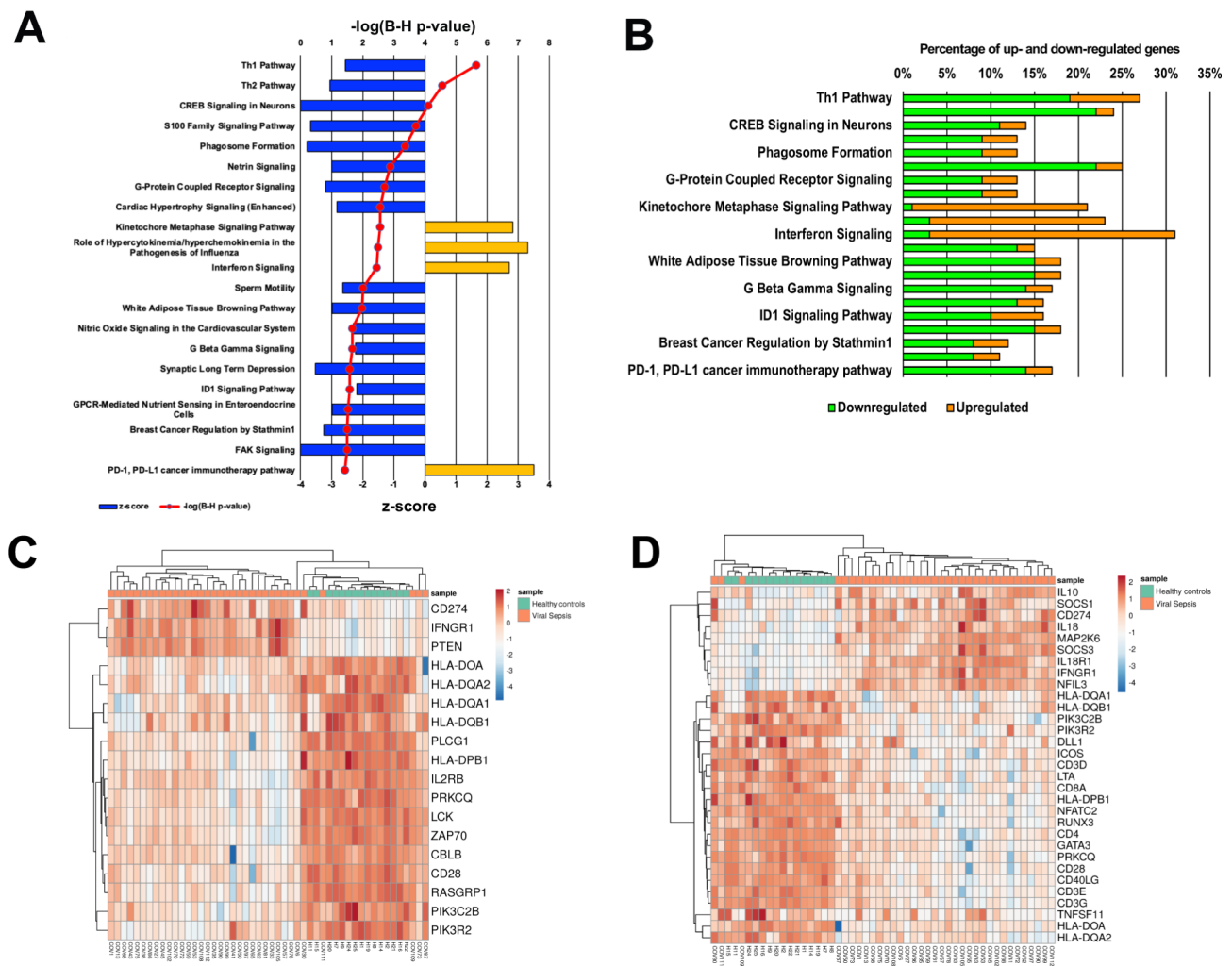


Fig. 4 Canonical pathway and heatmaps of mRNA in patients with viral (COVID-19) sepsis and healthy volunteers. **(A)** Canonical pathway analysis of patients with viral (COVID-19) sepsis and healthy volunteers. The bars represent z-scores, and the line graphs represent the adjusted p values associated with each pathway in the logarithm. **(B)** The percentage of genes up- and down-regulated in the pathways shown in panel A. These charts display the number of molecules in our dataset that belong to a significant pathway and show the proportions of upregulated (orange), and downregulated (green) molecules. **(C)** A heatmap of genes in the PD-1 and PD-L1 cancer immunotherapy pathways as representatives of the upregulated pathways, and how each gene is upregulated and downregulated. **(D)** A heatmap of genes in the Th1 pathway as a representative of downregulated pathways, and how each gene is up- and down-regulated

indicating a dynamic change in gene expression and pathway activation in bacterial sepsis (Fig. 2A-D). Our group previously reported that 28 pathways, including the IFN pathway, were activated and one pathway was inhibited in miRNA-targeted mRNA [7]. When we compared bacterial sepsis patients and viral (COVID-19) sepsis patients using an optimal threshold for bacterial sepsis patients (FDR: 0.05, $|\log_2FC| > 1.5$), we could not find changes in the various pathways in the viral (COVID-19) sepsis patients that were previously reported by our group [7]. As the optimal threshold for COVID-19 patients in this report [7] is FDR: 0.1 and $|\log_2FC| > 0.6$, the threshold in bacterial sepsis in this study (FDR: 0.05 and $|\log_2FC| > 1.5$) is more stringent than the optimal threshold for viral (COVID-19) sepsis patients, which may have influenced

this result. Thus, the optimal threshold for bacterial sepsis is substantially lower than that for viral (COVID-19) sepsis, indicating that bacterial sepsis causes a more dynamic change in the pathway (Figs. 3 and 4).

From previous research on differentially expressed miRNAs and long ncRNAs, they found that the TNF, MAPK, and NF- κ B signaling pathways are the most significantly changed pathways during recovery from COVID-19. These networks are closely linked with inflammatory factor genes TNF and IL-1 β , and transcription factor AP-1 subunit gene *JUN*. The AP-1 connected nodes were at the core of the enriched KEGG maps, including the Toll-like receptor (TLR) signaling pathway, IL-17 signaling pathway, and PD-L1 expression and PD-1 checkpoint pathway. The activation of AP-1

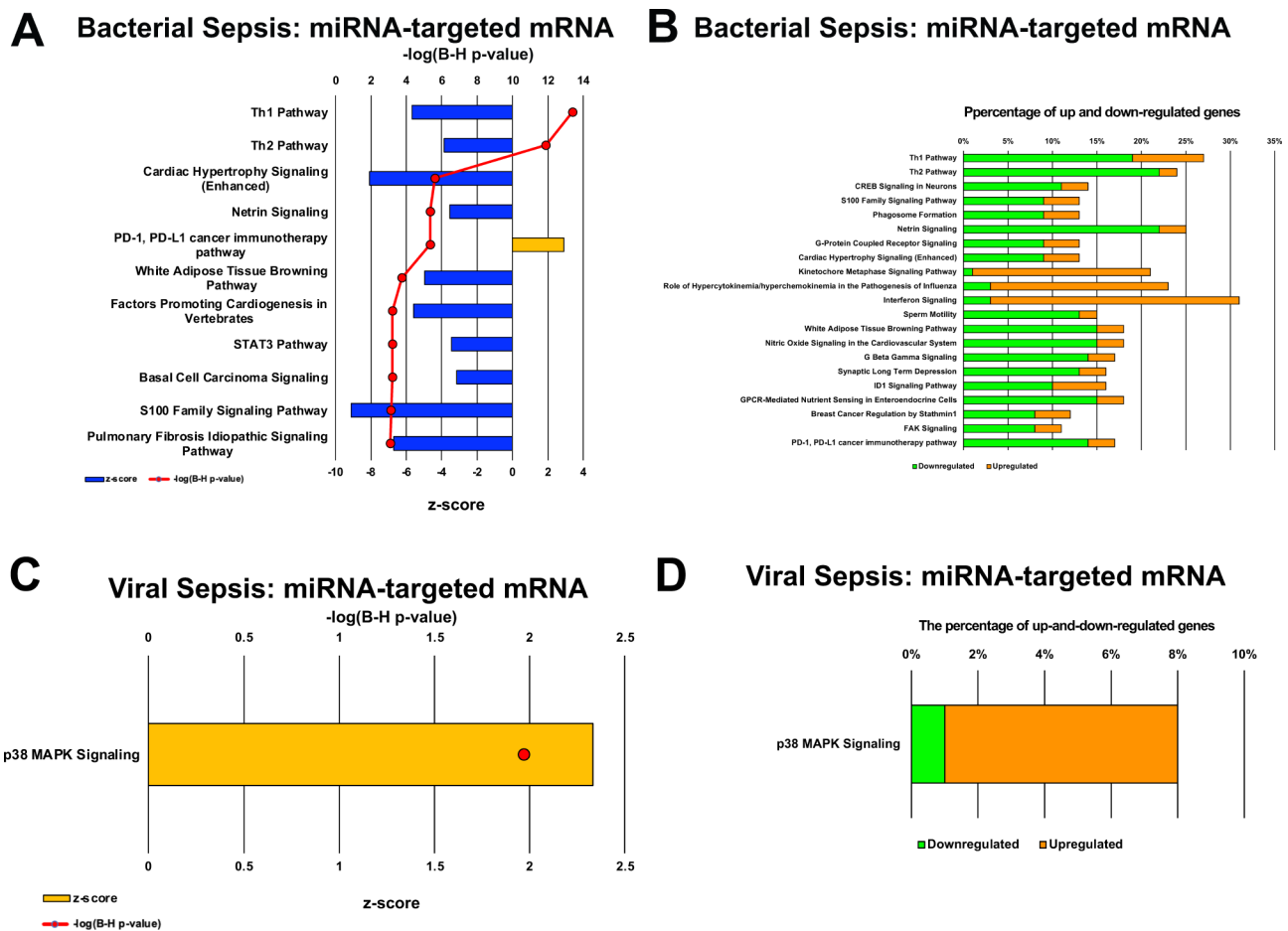


Fig. 5 Canonical pathway analysis and heatmaps of miRNA-targeted mRNAs. **(A)** Canonical pathway analysis of patients with bacterial sepsis and healthy volunteers. The bars represent z-scores, and the line graphs represent the adjusted p values associated with each pathway in the logarithm. **(B)** The percentage of genes up- and down-regulated in the pathways shown in panel A. **(C)** Canonical pathway analysis of patients with viral (COVID-19) sepsis and healthy volunteers. The bars represent z-scores, and the line graphs represent the adjusted p values associated with each pathway in the logarithm. **(D)** The percentage of genes up- and down-regulated in the pathways shown in panel C.

and NF- κ B signals caused increased expression of inflammatory factors such as TNF- α , IL-1 β , IL-8, MIP1 α , and MIP-1 β according to the KEGG enrichment analysis, which might be detrimental to COVID-19 rehabilitation [11]. Our study revealed the activation of the PD-1 and PD-L1 cancer immunotherapy signaling pathway and the concurrent suppression of Th1 signaling in the bacterial sepsis patients. In particular, Th1 signaling was more suppressed in bacterial sepsis than in viral (COVID-19) sepsis.

PD-1 and its ligands, PD-L1, act as receptors that modulate co-stimulatory and coinhibitory immune responses and play a critical role in regulating inflammatory responses during infections, autoimmunity, and allergies [12]. Notably, these pathways appear to be particularly significant in bacterial sepsis-induced immunosuppression, functioning as part of a negative feedback mechanism [13]. PD-L1 assumes a major role within the PD-1 and PD-L1 cancer immunotherapy signaling pathway

by exerting inhibitory effects, whereas PD-1 functions as an auxiliary component [14]. The observed activation of these pathways in our study suggests a dysregulation of the immune response, potentially contributing to the excessive inflammation and immune dysfunction observed in bacterial sepsis. Furthermore, the inhibition of Th1 signaling, which is crucial for cellular immune responses and inflammation control, supports the notion of immune response dysregulation in bacterial sepsis [6]. TBX21 (Fig. 6B, D), which is regulated in bacterial sepsis upstream regulator analysis, was also suppressed at a central position in the Th-1 pathway (Fig. S4). In contrast, TBX21 was not found in the upstream regulator analysis of the viral (COVID-19) sepsis patients (Fig. 7B, D). TBX21 works to cause Th progenitor cells to differentiate into Th1 effector cells [15–17]. Our study also confirmed that TBX21 is suppressed in the Th-1 pathway. Its suppression may represent the underlying immune dysfunction observed in bacterial sepsis. Figure S2A-H shows

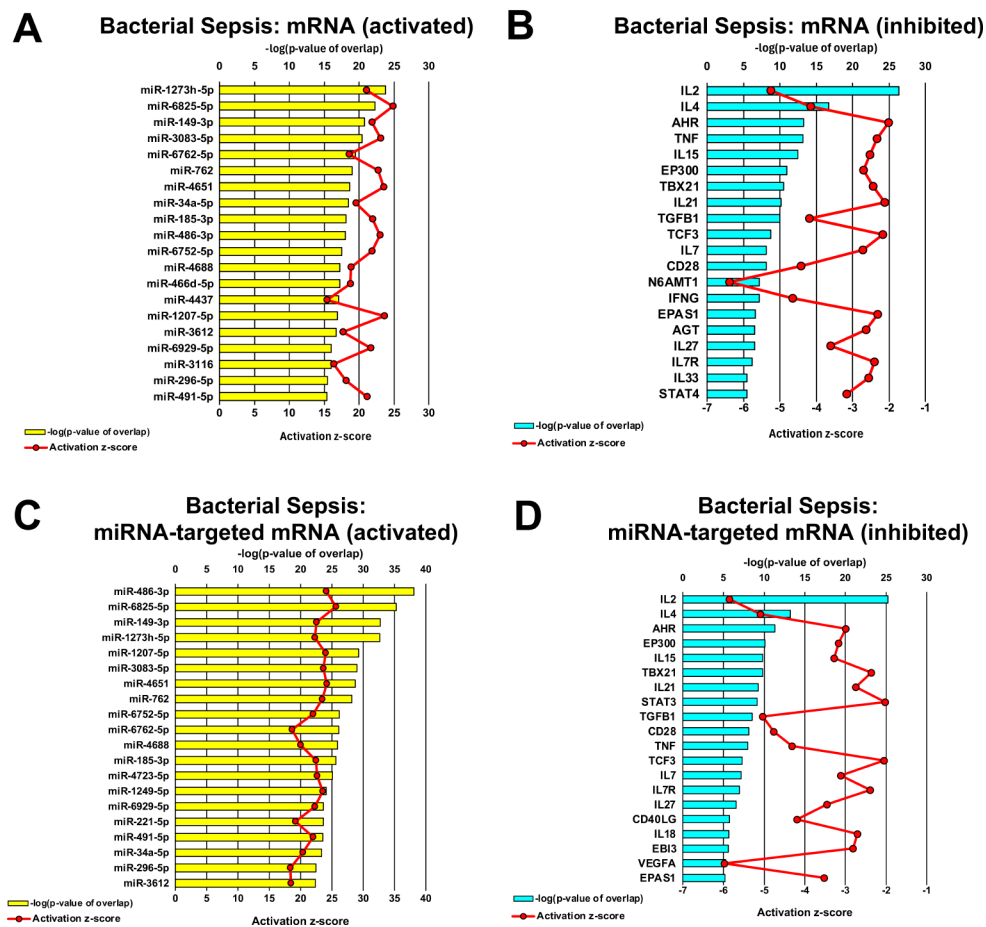


Fig. 6 Upstream regulator analysis of patients with bacterial sepsis and healthy volunteers. The bar graphs show the common logarithm of the overlap of p values of transcriptional regulators that differed in bacterial sepsis patients compared to healthy controls, and the line graphs show the z values. **(A)** Regulators that are active in patients with bacterial sepsis as inferred from significant alterations in mRNA expression profiles between septic patients and healthy controls. **(B)** Suppressed regulators identified through analysis of mRNA data. **(C)** Active regulators in the context of bacterial sepsis identified by analyzing mRNAs that are under the regulatory influence of miRNAs that exhibit differential gene expression patterns between septic and healthy individuals. **(D)** Downregulated regulators identified by the differential regulatory patterns of mRNAs by miRNAs in the context of bacterial sepsis

that similar results are confirmed for pathway analysis results other than IPA. Therefore, this result may be representative and indicative of the patient's immune status as previous studies and analyses in different sources have suggested similar pathway associations.

In a previous study, patients with bacterial sepsis showed more severe organ dysfunction and poorer outcomes compared to viral (COVID-19) sepsis patients [18]. This difference may be due to the fact that bacterial sepsis often causes systemic inflammation and multiorgan failure [19], whereas COVID-19 manifests primarily as respiratory dysfunction [20]. COVID-19 is characterized by respiratory symptoms. Approximately 15% of patients develop pneumonia, and 5% are critically ill due to respiratory failure from acute respiratory distress syndrome, shock, and/or multiorgan dysfunction. In later stages of the infection, when viral replication accelerates, epithelial-endothelial barrier integrity

is compromised. In addition to epithelial cells, SARS-CoV-2 infects pulmonary capillary endothelial cells, which accentuate the inflammatory response and trigger an influx of monocytes and neutrophils [21].

The differences observed in the number of genes expressed and altered in our study may reflect differences in the underlying disease mechanisms and pathophysiological processes of bacterial sepsis and COVID-19. In our study, we used whole blood RNA sequencing to reveal striking differences in gene expression and pathway activation between the bacterial sepsis patients and viral (COVID-19) sepsis patients.

There were no significant differences in the severity assessments as indicated by the APACHE II and SOFA scores between the patients with bacterial versus viral (COVID-19) sepsis. The following differences between bacterial and viral infections may account for the marked differences in gene expression in this study.

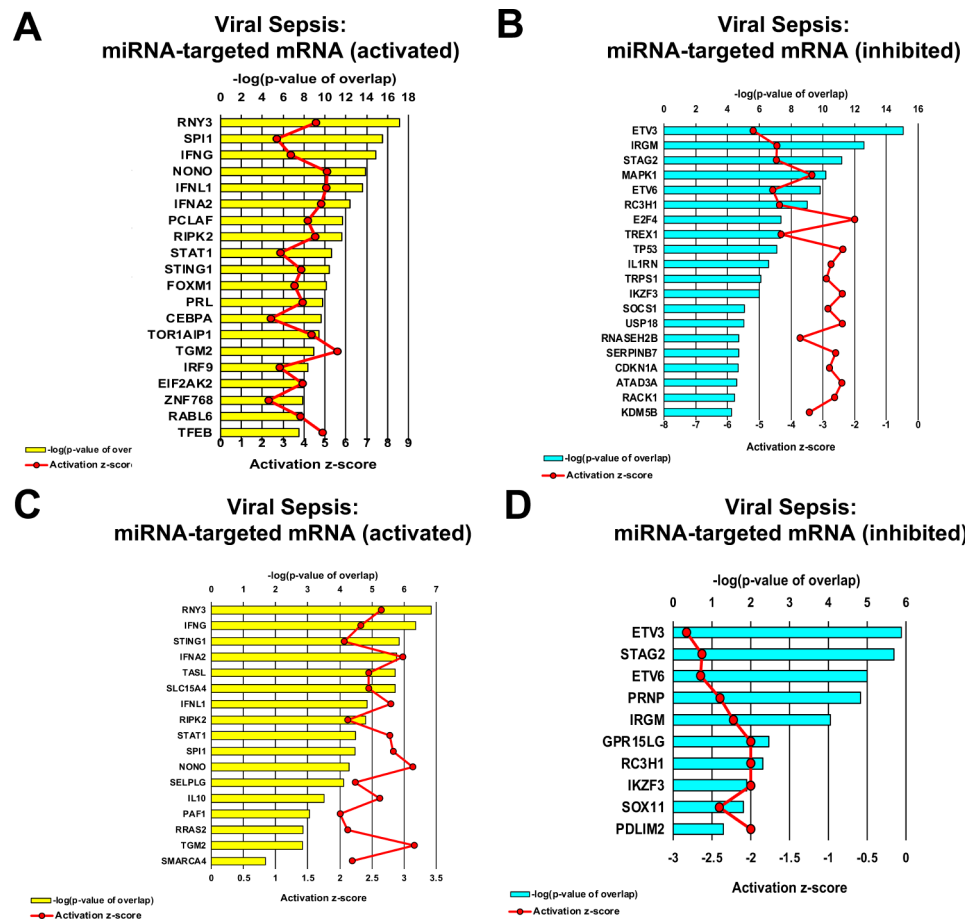


Fig. 7 Upstream regulator analysis of viral (COVID-19) sepsis patients and healthy volunteers. The bar graphs delineate the common logarithm of the adjusted p values corresponding to transcriptional regulators that manifested differential activity in viral (COVID-19) sepsis patients as compared to healthy controls. The line graphs simultaneously present the distribution of the corresponding z-scores. **(A)** Transcriptional regulators that are active in viral (COVID-19) sepsis patients as inferred from significant alterations in the gene expression profiles of mRNA between viral (COVID-19) sepsis patients and healthy controls. **(B)** Suppressed transcriptional regulators identified through the analysis of mRNA data. **(C)** Transcriptional regulators that are active in the context of viral (COVID-19) sepsis patients as determined by analyzing mRNAs that are under the regulatory influence of miRNAs with differential gene expression patterns between viral (COVID-19) sepsis patients and healthy individuals. **(D)** Downregulated transcriptional regulators identified by the differential regulatory patterns of mRNAs by miRNAs in the context of viral (COVID-19) sepsis patients

From a clinicopathologic viewpoint, bacterial sepsis causes severe systemic inflammation and multiorgan damage, and even septic shock in the early stages. In contrast, COVID-19 infections cause no apparent immunoinflammatory response in the early stages of invasion and may have an incubation period of 10 days or more. Even when respiratory compromise occurs, the general condition of most patients remains relatively stable, although some patients may suddenly become quite ill and even die.

From an immunological perspective, the difference between bacterial sepsis and viral sepsis, including COVID-19 infection, lies in the activation of pattern recognition receptors and TLRs [22]. In bacterial infections, TLR2 and TLR4 are primarily activated and recognize bacterial-derived lipopolysaccharide and peptidoglycans, which leads to a strong inflammatory response. In

viral infections, however, TLR3, TLR7, TLR8, and TLR9 recognize virus-derived RNA and DNA and induce interferon-mediated antiviral responses. Thus, it is suggested that bacterial and viral sepsis may have different host responses due to differences in pathogenic microorganisms.

Limitations

There are several limitations in this study. First, there is a significant difference in age between the bacterial sepsis patients, viral (COVID-19) sepsis patients, and healthy control subjects. Second, this is single-center study with a small number of participants, which can lead to reduced general validity of the results. Third, it is impossible to determine how they specifically affect the pathway. Consequently, a multicenter cohort study will be required for further validation of the results.

Conclusion

Our study revealed distinct molecular profiles between bacterial sepsis and viral (COVID-19) sepsis. Bacterial sepsis patients had a greater number of upregulated and downregulated genes and pathways compared to viral (COVID-19) sepsis patients. Especially, bacterial sepsis caused more dramatic pathogenetic changes in the Th1 pathway than did viral (COVID-19) sepsis.

Abbreviations

| | |
|------------|---|
| APACHE II | Acute Physiology and Chronic Health Evaluation II |
| DEGs | Differentially expressed genes |
| FDR | False discovery rate |
| GO | Gene Ontology |
| GSEA | Gene set enrichment analysis |
| IPA | Ingenuity Pathway Analysis |
| IQR | Interquartile range |
| KEGG | Kyoto Encyclopedia of Genes and Genomes |
| miRNAs | microRNAs |
| mRNA | messenger RNA |
| ncRNA | noncoding RNA |
| PCA | Principal component analysis |
| SARS-CoV-2 | Severe acute respiratory syndrome coronavirus 2 |
| SOFA | Sequential Organ Failure Assessment |
| TLR | Toll-like receptor |

Supplementary Information

The online version contains supplementary material available at <https://doi.org/10.1186/s12985-024-02451-6>.

Supplementary Material 1: Fig. S1 Principal component analysis (PCA) results. (A) PCA of total mRNAs between bacterial sepsis patients (shown as P), viral (COVID-19) sepsis patients (shown as COV), and healthy controls (shown as H). (B) PCA of total miRNA-targeted mRNAs between bacterial sepsis patients, viral (COVID-19) sepsis patients, and healthy controls.

Supplementary Material 2: Fig. S2 Results from two types of gene set enrichment analyses, Gene Ontology (GO) analyses and Kyoto Encyclopedia of Genes and Genomes (KEGG) pathway analyses. (A) GO analysis of mRNA in bacterial sepsis patients. (B) KEGG pathway analysis of mRNA in bacterial sepsis patients. (C) GO analysis of miRNA-targeted mRNA in bacterial sepsis patients. (D) KEGG pathway analysis of miRNA-targeted mRNA in bacterial sepsis patients.

Supplementary Material 3: Fig. S2 (E) GO analysis of mRNA in viral (COVID-19) sepsis patients. (F) KEGG pathway analysis of mRNA in viral (COVID-19) sepsis patients. (G) GO analysis of miRNA-targeted mRNA in viral (COVID-19) sepsis patients. (H) KEGG pathway analysis of miRNA-targeted mRNA in viral (COVID-19) sepsis patients.

Supplementary Material 4: Fig. S3 The activated PD-1 and PD-L1 cancer immunotherapy pathways predicted by Ingenuity Pathway Analysis. For $|\log_2 \text{fold change}| > 1.5$ and $\text{FDR} < 0.05$, 53 miRNAs were predicted to be involved in pathway regulation. FDR, false discovery rate

Supplementary Material 5: Fig. S4 The inhibited Th2 pathway predicted by Ingenuity Pathway Analysis. For $|\log_2 \text{Fold Change}| > 1.5$ and $\text{FDR} < 0.05$, 55 miRNAs were predicted to be involved in pathway regulation. FDR, false discovery rate

Acknowledgements

We greatly appreciate the patients and healthy volunteers who were involved in this study. We would also like to acknowledge the Academic Support Desk at Osaka University, and especially Dr. Neville Greening, for his invaluable assistance in our submission of this paper.

Author contributions

AM, Sayaka O, Sinya O, and JY contributed equally to this work. AM, Sayaka O, Shinya O, and JY conceived and designed this study, acquired the data, and analyzed and wrote the manuscript. HM helped with study design and data interpretation and conducted the literature review. YT, YM, and HI contributed to acquiring the data. DO helped analyze the data. HO and JO conducted the literature review. All authors have read and understood the journal's policies and believe that neither the manuscript nor the study violates any of these. All authors meet the authorship criteria detailed in the submission guidelines, and all authors agree with the content of the manuscript.

Funding

This study was supported by the Japan Agency for Medical Research and Development (grant no. 20fk0108404h0001) and The Nippon Foundation – Osaka University Project for Infectious Disease Prevention.

Data availability

The raw data concerning this study were submitted under Gene Expression Omnibus accession numbers GSE243219 for future access.

Declarations

Ethical approval

The study protocol was approved by the Institutional Review Board of Osaka University Hospital (Approval Number: 885 [Osaka University Critical Care Consortium Novel Omix Project; Occonomix Project]). Informed consent was obtained from the patients or their relatives and the healthy volunteers for the collection of all blood samples.

Consent for publication

Anonymized information was used, and no identifiable images were included in this study.

Competing interests

The authors declare no competing interests.

Author details

¹Department of Traumatology and Acute Critical Medicine, Osaka University Graduate School of Medicine, Osaka, Japan

²Department of Oral and Maxillofacial Surgery, Osaka University Graduate School of Dentistry, Osaka, Japan

³Laboratory for Human Immunology (Single Cell Genomics), WPI Immunology Frontier Research Center, Osaka University, Osaka, Japan

Received: 11 October 2023 / Accepted: 30 July 2024

Published online: 19 August 2024

References

- Hotchkiss RS, Monneret G, Payen D. Sepsis-induced immunosuppression: from cellular dysfunctions to immunotherapy. *Nat Rev Immunol*. 2013;13(12):862–74. <https://doi.org/10.1038/nri3552>.
- Maharaj R, McGuire A, Street A. Association of annual intensive care unit sepsis caseload with hospital mortality from sepsis in the United Kingdom, 2010–2016. *JAMA Netw Open*. 2021;4(6):e2115305. <https://doi.org/10.1001/jamanetworkopen.2021.15305>.
- Bhatraju PK, Ghassemieh BJ, Nichols M, Kim R, Jerome KR, Nalla AK, et al. Covid-19 in critically ill patients in the Seattle region – case series. *N Engl J Med*. 2020;382(21):2012–22. <https://doi.org/10.1056/NEJMoa2004500>.
- Stefani G, Slack FJ. Small non-coding RNAs in animal development. *Nat Rev Mol Cell Biol*. 2008;9(3):219–30. <https://doi.org/10.1038/nrm2347>.
- Lu J, Getz G, Miska EA, Alvarez-Saavedra E, Lamb J, Peck D, et al. MicroRNA expression profiles classify human cancers. *Nature*. 2005;435(7043):834–8. <https://doi.org/10.1038/nature03702>.
- Singer M, Deutschman CS, Seymour CW, Shankar-Hari M, Annane D, Bauer M, et al. The Third International Consensus definitions for Sepsis and septic shock (Sepsis-3). *JAMA*. 2016;315(8):801–10. <https://doi.org/10.1001/jama.2016.0287>.
- Togami Y, Matsumoto H, Yoshimura J, Matsubara T, Ebihara T, Matsuura H, et al. Significance of interferon signaling based on mRNA-microRNA integration

- and plasma protein analyses in critically ill COVID-19 patients. *Mol Ther Nucleic Acids*. 2022;29:343–53. <https://doi.org/10.1016/j.omtn.2022.07.005>.
8. Koschmann J, Bhar A, Stegmaier P, Kel A, Wingender E. Upstream Analysis: an integrated promoter-pathway analysis approach to causal interpretation of microarray data. *Microarrays*. 2015;4(2):270–86. <https://doi.org/10.3390/microarrays4020270>.
 9. Law CW, Chen Y, Shi W, Smyth GK. Voom: Precision weights unlock linear model analysis tools for RNA-seq read counts. *Genome Biol*. 2014;15(2):R29. <https://doi.org/10.1186/gb-2014-15-2-r29>.
 10. Dong X, Wang C, Liu X, Gao W, Bai X, Li Z. Lessons learned comparing immune system alterations of bacterial sepsis and SARS-CoV-2 sepsis. *Front Immunol*. 2020;11:598404. <https://doi.org/10.3389/fimmu.2020.598404>.
 11. Zheng HY, Xu M, Yang CX, Tian RR, Zhang M, Li JJ, et al. Longitudinal transcriptome analyses show robust T cell immunity during recovery from COVID-19. *Signal Transduct Target Ther*. 2020;5(1):294. <https://doi.org/10.1038/s41392-020-00457-4>.
 12. Galván Morales MA, Montero-Vargas JM, Vizuet-de-Rueda JC, Teran LM. New insights into the role of PD-1 and its ligands in allergic disease. *Int J Mol Sci*. 2021;22(21):11898. <https://doi.org/10.3390/ijms222111898>.
 13. Monneret G, Gossez M, Venet F. Sepsis in PD-1 light. *Crit Care*. 2016;20(1):186. <https://doi.org/10.1186/s13054-016-1370-x>.
 14. Han Y, Liu D, Li L. PD-1/PD-L1 pathway: current researches in cancer. *Am J Cancer Res*. 2020;10(3):727–42.
 15. Oh S, Hwang ES. The role of protein modifications of t-bet in cytokine production and differentiation of T helper cells. *J Immunol Res*. 2014;2014:1–7. <https://doi.org/10.1155/2014/589672>.
 16. Szabo SJ, Kim ST, Costa GL, Zhang X, Fathman CG, Glimcher LH. A novel transcription factor, T-bet, directs Th1 lineage commitment. *Cell*. 2000;100(6):655–69. [https://doi.org/10.1016/S0092-8674\(00\)80702-3](https://doi.org/10.1016/S0092-8674(00)80702-3).
 17. Lazarevic V, Glimcher LH. T-bet in disease. *Nat Immunol*. 2011;12(7):597–606. <https://doi.org/10.1038/ni.2059>.
 18. Ren C, Yao RQ, Ren D, Li Y, Feng YW, Yao YM. Comparison of clinical laboratory tests between bacterial sepsis and SARS-CoV-2-associated viral sepsis. *Military Med Res*. 2020;7(1):36. <https://doi.org/10.1186/s40779-020-00267-3>.
 19. Caraballo C, Jaimes F. Organ dysfunction in sepsis: an ominous trajectory from infection to death. *Yale J Biol Med*. 2019;92(4):629–40.
 20. Su WL, Lu KC, Chan CY, Chao YC. COVID-19 and the lungs: a review. *J Infect Public Health*. 2021;14(11):1708–14. <https://doi.org/10.1016/j.jiph.2021.09.024>.
 21. Wiersinga WJ, Rhodes A, Cheng AC, Peacock SJ, Prescott HC. Pathophysiology, transmission, diagnosis, and treatment of coronavirus disease 2019 (COVID-19): a review. *JAMA*. 2020;324(8):782. <https://doi.org/10.1001/jama.2020.12839>.
 22. Akira S, Uematsu S, Takeuchi O. Pathogen recognition and innate immunity. *Cell*. 2006;124(4):783–801. <https://doi.org/10.1016/j.cell.2006.02.015>.

Publisher's Note

Springer Nature remains neutral with regard to jurisdictional claims in published maps and institutional affiliations.